

# A Fast Self-calibration Method of Camera with Varying Intrinsic Parameters based on Vanishing Points

Mounir El Maghraoui<sup>1</sup><sup>a</sup>, Ismail El Batteoui<sup>1</sup><sup>b</sup>, Abderahim Saaidi<sup>2</sup><sup>c</sup> and Khalid Satori<sup>1</sup><sup>d</sup>

<sup>1</sup> LIAN Lab, Faculty of sciences Dhar-Mahraz B.P 1796 Atlas, University of Sidi Mohamed Ben Abdellah Fez, Morocco

<sup>2</sup>LIMAO Lab, Faculty of polydisciplinaire, University of Sidi Mohamed Ben Abdellah Fez, Morocco

**Keywords:** Unknown Scene, Vanishing Points, Variable intrinsic Parameters, Variable Extrinsic Parameters, Homography of the Plane at Infinity.

**Abstract:** In this article, we present a flexible and fast self-calibration system of camera from uncalibrated images taken by a mobile camera, characterized by variable intrinsic parameters. We propose a new method leveraging the Characteristics Particular Vanishing Points. The estimation of the extrinsic and intrinsic parameters of the camera was performed using only two frames, illustrating the importance of our method in terms of turnaround time. This shows the importance of our approach in terms of execution time. The principal reason for this method is the exploitation of the homography matrix induced by the plane at infinity. The identification is made by using two pairs of vanishing points between the two images. Which would allow us to formulate nonlinear equations according to the camera intrinsic parameters. The experimental results shown in this paper demonstrate that our algorithm is robust.


## 1 INTRODUCTION


Self-calibration is an important area of computer vision. Many applications based on this field are already utilized in medicine (medical imaging, surgical applications), 3D reconstruction to cite a few. So much literature already exist that describes Camera self-calibration. The latter can be realized in two manners: Self-calibration with constant parameters and self-calibration using variable intrinsic parameters. Our approach falls into the latter category. In fact, we have performed an auto-calibration on a camera having variable intrinsic parameters but with no prior knowledge of the subject and with fewer constraints (the number of images used, the characteristics of the cameras and the type of scene). This new solution does not necessitate any constraint on the scene or on the cameras. In addition, it minimizes the limitations of the self-calibration system.


In this work, we describe a new method for the self-calibration of cameras with variable intrinsic parameters, using an unknown 3D scene and two frames.


Our method based on the use of vanishing points to perform autocalibration. Calculates the homography from the detected vanishing points. It is assumed that Vanishing Point1 and Vanishing Point 2 (referred to as vp1 and vp2 in this paper) correspond to horizontal and vertical directions, although the order does not need to be respected.

Firstly, Projective Transform is computed to make the vanishing points go to infinity so that we have a Fronto Parellel view. Then, Affine Transform is computed to make axes corresponding to vanishing points orthogonal. The extraction of two vanishing points and the compute of the homography to infinity are exploited to formulate a nonlinear cost function. The downscaling of the operation by the Levenberg Marquardt algorithm (Moré, 1978) requires the evaluation of the intrinsic parameters of the devices used.

<sup>a</sup>  <https://orcid.org/0000-0000-0000-0000>

<sup>b</sup>  <https://orcid.org/0000-0000-0000-0000>

<sup>c</sup>  <https://orcid.org/0000-0000-0000-0000>

<sup>d</sup>  <https://orcid.org/0000-0000-0000-0000>

The article is divided into the form of the following sections: In section 2, we look at most of the self-calibration procedures and work that has been accomplished in recent studies. In section 3, we will study the basic structure of the camera model and the camera self-calibration tools. Section 4 will present the method we propose for camera self-calibration. In part 5, we will describe the framework used to evaluate the efficiency of the method. Lastly, section 6 will be a conclusion.

## 2 PRVIOUS WORK

Camera self-calibration consists in establishing the parameters of the mapping between the co-ordinates of the 3D scene and the co-ordinates of the image, and the other way around by an unknown scene.

We present in this part the two categories of existing methods of camera autocalibration: the first method concerns the autocalibration of cameras with constant intrinsic parameters. However, the second is called autocalibration of cameras with varying intrinsic parameters. At the beginning, we present methods based on the use of cameras characterized by constant intrinsic parameters. Next, we deal with methods based on the use of cameras with variable intrinsic parameters in order to deepen this type of approach.

Several research studies have also been carried out in this area.

(Triggs, 1998), suggests a method relying on the self-calibration of cameras with constant intrinsic parameters by a planar scene. The basic approach of this method is the prediction of these parameters by the projection of two pixels in each image, and the establishment of the homography between the different frames (at least five images).

(Strum, 2002), explores a technique based on the displacement of the camera which is based on constant intrinsic properties, with the notable exception of the focal length, which varies freely between the different views.

(Gurdjos and Sturm, 2003), explains an auto-calibration of the zoom camera from the frames of a plane scene whose Euclidean structure is unknown, the main idea of this method is to calculate both the intrinsic parameters of the camera and those related to the Euclidean pattern of the viewed scene, the formulation of the cost function is non-linear, which poses the problems of initialization of the focal length. In order to solve these difficulties, the authors have suggested a new specification that is not related to the focal length.

(Liu and Shi, 2003) offers a model that calculates the initial computation of the intrinsic and extrinsic parameters of the camera using some geometric constraints on the initial image, and the use of the additional image allows the optimization of the first solution.

(Cao and Xiao, 2006) investigates a further method complementary to the self-calibration of cameras with variable intrinsic partners from sequences of images of an object, this method is based on a constant motion between the images of the object moving around a single axis, the relationship between the projection matrices and those of the fundamental matrices yields the parameters of the camera by solving a system of non-linear equations.

(Saaidi and Halli, 2008), offers a method based on an unknown 3D scene to calibrate the camera with fixed intrinsic parameters. A non-linear cost function is formulated from a "translation and small rotation" motion of the camera to estimate the homography matrices of the infinite plane between the pair of images; and the solver of a linear cost function is used to obtain the estimation of the camera parameters.

(Zhao and Lv, 2012), wrote a self-calibration approach for cameras with constant intrinsic parameters using the creep line, the main idea of this method is to calculate the creep line by solving three linear equations based on circles and their centers. The respective values and theory of these circular lines and points are used to calculate the intrinsic parameters of the camera.

(Shang and Yue, 2012), proposes a method based on the relative distance of the scene and on the homography matrix that converts the projective reconstruction into measurement, the elements of which depend on the intrinsic parameters of the camera. These settings and the 3D structure are obtained by minimizing an error function related to the relative distance.

(Jiang and Liu, 2012), has introduced a self-calibration method for cameras with variable intrinsic parameters, relying on a quasi-affine reconstruction. After this reconstruction, the homography of the plane at infinity can be determined, and used with constraints on the image of the absolute conic to estimate the intrinsic properties of the cameras used.

(Zhao and Hu, 2012), presents a method based on round points which are obtained from the properties of the three prism, the intrinsic parameters of the camera can be determined linearly after the trailing points of each edge of the tri-prism and the coordination's of the round points have been calculated.

(Kluger and Ackermann, 2017).proposed a method of Deep learning for vanishing point detection using an inverse gnomonic projection.

(El Akkad and Merras, 2018) put forward a method for self-calibrating the camera using varying intrinsic factors based on a sequence of images of an unidentified 3D object.

### 3 SCORING AND TOOLS

#### 3.1 Rating

We consider a point  $P(X Y Z)^T$  of the 3D scene and its projection  $p = (u v)^T$  in the image either  $p_\infty = (u_\infty v_\infty)^T$  designates a point in the image plane, which represents the projection of a point at infinity  $P_\infty = (X_\infty Y_\infty Z_\infty)^T$ . We denote by  $\tilde{P}(X Y Z 1)^T$ ;  $\tilde{P}_\infty = (X_\infty Y_\infty Z_\infty 0)^T$ ;  $\tilde{p} = (u v 1)^T$  and  $\tilde{p}_\infty = (u_\infty v_\infty 1)^T$  the homogeneous coordinates of the points  $P, P_\infty, p$  and  $p_\infty$  respectively.

$O(0 0 0)^T$  The null vector,  $I_3$  the identity matrix  $3 \times 3$ .

#### 3.2 Modeling the Camera

Modeling a camera amounts to modeling the process of image formation, i.e. finding the relationship between the spatial coordinates of a point in space with the associated point in the image taken by the camera. In this section, we first describe the pinhole model. What is called pinhole corresponds to the center of the camera through which any light ray passes in a rectilinear fashion. The model depends on two sets of parameters: intrinsic and extrinsic. All of the intrinsic parameters shape the sensor's internal geometry and operational properties. The second set contains the extrinsic parameters that link the sensor frame to the frame associated with the scene where the reference objects useful for autocalibration are located.

Shows the pinhole camera model that we will use in this work to project points from the 3D scene into image planes.

We denote by  $K_i(R_i t_i)$  the matrix  $(3 \times 4)$  which characterizes this model, such as:

$$\tilde{p}_k \sim K_i[R_i t_i]\tilde{P}_k \quad (1)$$

$$K_i = \begin{pmatrix} f_i & s_i & u_{0i} \\ 0 & \varepsilon_i f_i & v_{0i} \\ 0 & 0 & 1 \end{pmatrix} \quad (2)$$

Where:  $\varepsilon_i$  is the scaling factor,  $f_i$  is the focused distance,  $s_i$  is the skew factor and  $(u_{0i} v_{0i})$  are the coordinates of the main focus point.

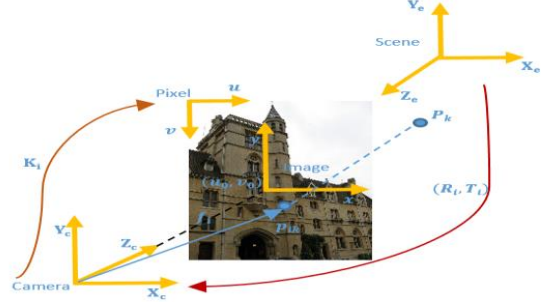


Figure 1: Projection of a scene point by the pinhole camera model.

#### 3.3 Infinity Homography

If we take, a point  $P_k^\infty$  of the 3D scene projected into the image planes 1 and  $i + 1$  by the following equations:

$$\rho_{0k\infty}\tilde{p}_{0k\infty} = K_0(I_3 \ 0)\tilde{P}_{k\infty} \quad (3)$$

$$\rho_{ik\infty}\tilde{p}_{ik\infty} = K_i(R_i \ t_i)\tilde{P}_{k\infty}, i \geq 1 \quad (4)$$

If we replace the value of  $\tilde{P}_{k\infty}$  in eq. (4), we get:

$$\begin{aligned} \rho_{0k\infty}\tilde{p}_{0k\infty} &= K_0(I_3 \ 0)(x_{k\infty} \ y_{k\infty} \ z_{k\infty} \ 0)^T \\ &= K_0(x_{k\infty} \ y_{k\infty} \ z_{k\infty})^T \end{aligned}$$

So:

$$(x_{k\infty} \ y_{k\infty} \ z_{k\infty})^T = \rho_{0k\infty}K_0^{-1}\tilde{p}_{0k\infty}$$

Likewise, if we replace the value of  $\tilde{P}_{k\infty}$  in eq. (5), we get:

$$(x_{k\infty} \ y_{k\infty} \ z_{k\infty})^T = \rho_{ik\infty}R_i^{-1}K_i^{-1}\tilde{p}_{ik\infty}$$

From these last equations, we can write:

$$\tilde{p}_{ik\infty} \sim K_i R_i K_0^{-1} \tilde{p}_{0k\infty} \quad (5)$$

So:

$$H_{i\infty} \sim K_i R_i K_0^{-1}, i \geq 1 \quad (6)$$

$H_{i\infty}$  It is the homography of the plane at infinity between images 1 and  $i+1$ .

#### 3.4 Vanishing Points

- Synopsis of approach

The most accurate method shown uses line detection (LSD), followed by RANSAC to find vanishing point hypotheses for those lines, and finally J-linkage (Toldo and Fusiello, 2008) to cluster the lines which had similar responses to the hypotheses. The consistency measure, which defines the quality of a VP for a given line, is the distance of a segment's endpoint to a line connecting its midpoint with a hypothetical VP, as described in (Wildenauer and Vincze, 2007).

- Key assumptions

This makes no "Manhattan world assumption" (under which images would be assumed to have three dominant vanishing points on a regular grid). Instead, a RANSAC variant (Wang and Zheng, 2008) or (Zhang, 2006) tries to detect the underlying number of models. There is no orthogonality restriction or correction on VPs. There is also no reliance on known camera parameters.

### 3.5 Image of the Absolute Conic

The perfect conic  $\Omega_\infty$  is a specific conic in the Infinite Plane. The conic  $\Omega_\infty$  is invariant to rigid displacements and smooth changes of scale, so that its relative position with respect to a moving camera is constant. Therefore, its image  $\omega$  will be constant if the intrinsic parameters of the camera are constant.

The conic  $\Omega_\infty$  can be considered as a calibration object present in all the scenes. The conic  $\Omega_\infty$  can be represented by the Dual Absolute Quadric  $\Omega'_\infty$ . In this instance,  $\Omega'_\infty$  and its carrying plane, the plane of infinity  $\Pi$ , are described by a geometric entity and the relationship between the  $\Omega'_\infty$  is conveniently provided by using the projection equation of the  $\Omega'_\infty$ :

$$\omega_i \approx P_i \Omega'_\infty P_i^T \quad (7)$$

The  $\Omega'_\infty$  can be shifted between pictures through the homography of his plane (i.e. the plane to the infinite).

From (2) we can write:

$$R_i = K_i^{-1} H_{i\infty} K_0$$

The rotation matrix  $R_i$  is orthogonal then:

$$R_i = R_i^{-T} \quad (8)$$

From where

$$K_i^{-1} H_{i\infty} K_0 = K_i^T H_{i\infty}^{-T} K_0^{-T}$$

Which give:

$$\omega_i = H_{i\infty}^{-T} \omega_0 H_{i\infty}^{-1} \quad (9)$$

$$\text{where } \omega_i = \begin{pmatrix} \omega_{i00} & \omega_{i01} & \omega_{i02} \\ \omega_{i10} & \omega_{i11} & \omega_{i12} \\ \omega_{i20} & \omega_{i21} & \omega_{i22} \end{pmatrix} = (K_i K_i^T)^{-1}$$

is the image of the absolute conic.

$$\omega_{i00} = \frac{1}{f_i^2}, \omega_{i01} = \omega_{i10} = -\frac{s_i}{\varepsilon_i f_i^3},$$

$$\omega_{i02} = \omega_{i20} = \frac{u_{0i} s_i - \varepsilon_i u_{0i} f_i}{\varepsilon_i f_i^3}$$

$$\omega_{i11} = \frac{s_i^2}{\varepsilon_i^2 f_i^4} + \frac{1}{\varepsilon_i^2 f_i^2},$$

$$\omega_{i12} = \omega_{i21} = -\frac{s_i (v_{0i} s_i - u_{0i} \varepsilon_i f_i)}{\varepsilon_i^2 f_i^4} - \frac{v_{0i}}{\varepsilon_i^2 f_i^2}$$

$$\omega_{i22} = \frac{(v_{0i} s_i - u_{0i} \varepsilon_i f_i)^2}{\varepsilon_i^2 f_i^4} + \frac{v_{0i}^2}{\varepsilon_i^2 f_i^2} + 1,$$

The infinite point of a line defines its direction by  $P_\infty^{(1)}, P_\infty^{(2)}$ , so it respectively, let respectively be the infinite points of two orthogonal lines, and then we have  $(P_\infty^{(1)})^T \Omega_\infty P_\infty^{(2)} = 0$  since two orthogonal directions is a pair of points conjugated with respect to the absolute conic. Thus, the image points  $\tilde{p}^{(1)}, \tilde{p}^{(2)}$  of  $P_\infty^{(1)}, P_\infty^{(2)}$ , called vanishing points of orthogonal directions, satisfy the following equation:

$$(\tilde{p}^{(1)})^T K^{-T} K^{-1} \tilde{p}^{(2)} = 0 \quad (10)$$

## 4 PROPOSED METHOD

In this section, we will describe in detail our autocalibration method proposed in this paper.

To do this, we will start by detecting the points of interest, then the mapping of these points implemented and we end with the step of formulating the self-calibration equations based on the use of vanishing points.

### 4.1 Autocalibration Equations

$$\text{We pose: } \omega_j = \begin{pmatrix} \omega_{j00} & \omega_{j01} & \omega_{j02} \\ \omega_{j10} & \omega_{j11} & \omega_{j12} \\ \omega_{j20} & \omega_{j21} & \omega_{j22} \end{pmatrix}$$

And

$$H_{i\infty}^{-T} \omega_0 H_{i\infty}^{-1} = \omega'_i = \begin{pmatrix} \omega'_{i00} & \omega'_{i01} & \omega'_{i02} \\ \omega'_{i10} & \omega'_{i11} & \omega'_{i12} \\ \omega'_{i20} & \omega'_{i21} & \omega'_{i22} \end{pmatrix}$$

From (9) we deduce the following five equations:

$$\omega_{j00} \omega'_{i01} - \omega_{j01} \omega'_{i00} = 0$$

$$\omega_{j01} \omega'_{i02} - \omega_{j02} \omega'_{i01} = 0$$

$$\omega_{j02} \omega'_{i11} - \omega_{j11} \omega'_{i02} = 0$$

$$\omega_{j11} \omega'_{i12} - \omega_{j12} \omega'_{i11} = 0$$

$$\omega_{j12} \omega'_{i22} - \omega_{j22} \omega'_{i12} = 0$$

Equations (9) and (10) give:

$$\tilde{v}'_1 K_0^{-T} K_0^{-1} \tilde{v}'_2 = 0, \tilde{v}'_1 K_0^{-T} K_0^{-1} \tilde{v}'_3 = 0$$

$$\tilde{v}'_2 K_0^{-T} K_0^{-1} \tilde{v}'_3 = 0, \tilde{v}'_{1i} K_i^{-T} K_i^{-1} \tilde{v}'_{2i} = 0, i \geq 1$$

$$\tilde{v}'_{1i} K_i^{-T} K_i^{-1} \tilde{v}'_{3i} = 0, i \geq 1, \tilde{v}'_{2i} K_i^{-T} K_i^{-1} \tilde{v}'_{3i} = 0, i \geq 1$$

$$\omega'_{i00} \omega_{j01} - \omega'_{j01} \omega_{i00} = 0, \omega'_{i01} \omega_{j02} - \omega'_{j02} \omega_{i01} = 0$$

$$\omega'_{i02} \omega_{j11} - \omega'_{j11} \omega_{i02} = 0, \omega'_{i11} \omega_{j12} - \omega'_{j12} \omega_{i11} = 0$$

$$\omega'_{i12} \omega_{j22} - \omega'_{j22} \omega_{i12} = 0$$

The previous expression is nonlinear it contains eleven equations with unknowns of teeth: five for  $\omega_0$  and a fifth for  $\omega_i$  so, to satisfy it, we estimate the nonlinear cost function by the Levenberg-Marquardt algorithm (Moré, 1978):

$$\min_{\omega_0, \omega_i} \sum_{i=1}^n \alpha^2 + \vartheta^2 + \epsilon^2 + \beta_i^2 + \lambda_i^2 + \mu_i^2 + \gamma_i^2 + \delta_i^2 + \tau_i^2 + \rho_i^2 + \chi_i^2 \quad (11)$$

With:

$$\alpha = \tilde{v}'_1 K_0^{-T} K_0^{-1} \tilde{v}'_2, \vartheta = \tilde{v}'_1 K_0^{-T} K_0^{-1} \tilde{v}'_3$$

$$\epsilon = \tilde{v}'_2 K_0^{-T} K_0^{-1} \tilde{v}'_3, \beta_i = \tilde{v}'_{1i} K_j^{-T} K_j^{-1} \tilde{v}'_{2i}$$

$$\lambda_i = \tilde{v}'_{1i} K_j^{-T} K_j^{-1} \tilde{v}'_{3i}, \mu_i = \tilde{v}'_{2i} K_j^{-T} K_j^{-1} \tilde{v}'_{3i}$$

$$\gamma_i = w_{11} w'_{12i} - w_{12} w'_{11i}$$

$$\delta_i = w_{12} w'_{13i} - w_{13} w'_{12i}$$

$$\tau_i = w_{13} w'_{22i} - w_{22} w'_{31i}$$

$$\rho_i = w_{22} w'_{23i} - w_{23} w'_{22i}$$

$$\chi_i = w_{23} w'_{33i} - w_{33} w'_{23i}$$

We are going to calculate the intrinsic matrices from three orthogonal vanishing points for each image, the values obtained are focal distance, coordinates of principal point for each image, which will be the initial values of our system of nonlinear equations, which requires an initialization step.

## 4.2 Rotation Matrix

After the focal length being calculated, the direction vectors  $\vec{d}_{ox}$  and  $\vec{d}_{oy}$  can be computed. Let  $\vec{d}_z = \vec{d}_{ox} \times \vec{d}_{oy}$ , and making  $\vec{d}_z$  as the third axis, a coordinate frame can be constructed at the corner structure. The point O is the original point; OX and OY are the x-axis and y-axis separately and  $\vec{d}_z$  is the z-axis. We call this constructed coordinate frame SCF. The representation matrix of SCF in the camera coordinate frame can be written as:

$r = [\vec{d}_{ox} \ \vec{d}_{oy} \ \vec{d}_z]$ , where r is a 3×3 matrix and each column of r is an axis direction of SCF.

## 4.3 Translation Vector

Once the focal length known, the direction of the translation vector can be denoted as  $\vec{t}_{id} = [x_0 \ y_0 \ f]$ . Since the corner structure in two images will be used in the following optimization, the two translation vectors of the two cameras have to be balanced. Let  $\vec{V}_{ox} = [1 \ 0 \ 0]^T$  denotes the unit direction vector of OX in SCF. Reviewing the projection equation of pin-hole camera model, the projection of X can be written as:  $s * r_1 * (\vec{V}_{ox} - \lambda * r_1^T * \vec{t}_{id})$ , it is an equations set which includes three equations and there are two unknown values: s and  $\lambda$ . The value of s can be calculated from the third equation and then the least squares solution of  $\lambda$  can be calculated from the other two equations. Then the translation vector of the first camera is calculated:  $\vec{t}_1 = \lambda * \vec{t}_{id}$ , The same process is done to the second camera and  $\vec{t}_2$  is computed. Up to now, the focal length and all the extrinsic parameters have been recovered and the next step is to optimize the solution and make them more precise.

## 5 EXPERIMENTS

### 5.1 Synthetic Data

We have done several experiments with our algorithm and two of them are shown here. Fig 2 shows two synthetically images of a box, the real values of the two cameras and the calculated ones are represented in Table 1. We define the relative calibration error of the focal length as  $e_f = \|\tilde{f} - f\|/\|f\|$ , the relative calibration error of the rotation matrix as  $e_R = \|\tilde{R} - R\|/\|R\|$ , the relative error of the translation vector as  $e_t = \|\tilde{t} - t\|/\|t\|$ . The relative errors of the calculated parameters are shown in Table 2. From Table 2 we can see that the relative errors are quite little.

### 5.2 Real Data

Our self-calibration procedure using the York Urban Dataset is shown in Figure 3. The evaluation of the intrinsic parameters of the camera in the images  $\{I_0, I_n\}_{1 \leq n \leq m}$  is given by minimizing the cost feature (11) using the Levenberg-Marquardt algorithm. To estimate the intrinsic parameters of each camera by our approach, two phases must be implemented: initialization to generate an immediate solution and reduction of the cost element in order to find an ideal solution. The scene consists of several points; the projection is done according to the pinhole model.



Figure 2: Two synthetically images of a box.

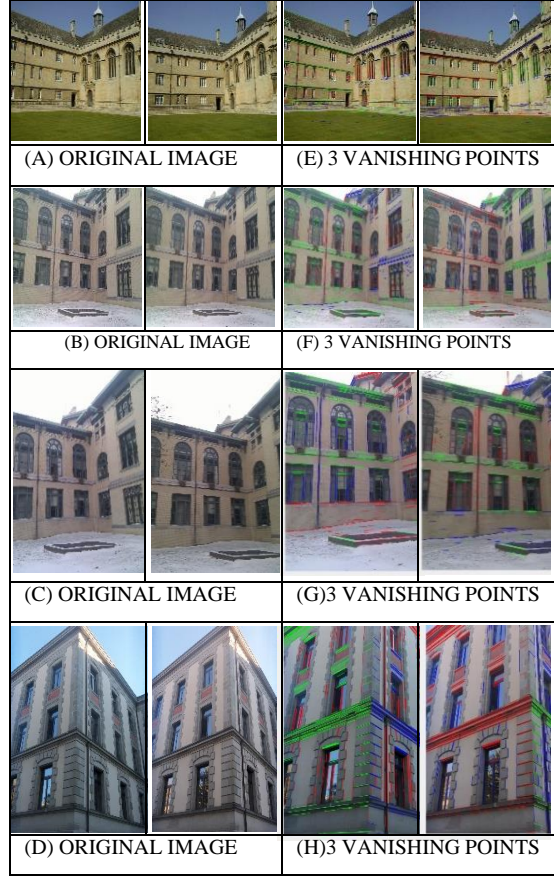


Figure 3: An illustration of vanishing point estimation results three orthogonal vanishing points on a selfcalibrated image in Manhattan world, original(A, B, C, D), three vanishing points (E, F, G, H).

Table 1: The results of the first experiment.

	Focal length $f$	Angle round x-axis		Angle round y-axis		Angle round z-axis	
<b>Real</b>	800.0	0		20		0	
<b>Calculated</b>	802,3	0,3		19.5		0.5	
	816.8						
		x-translation (pixels)		y-translation (pixels)		z-translation (pixels)	
		x	x/z	y	y/z	z	z/z
<b>Real</b>	ts1	4683.01	-1.30	-1776.19	0.49	-3608.49	1
	ts2	6598.08	-3.22	-1107.88	0.54	-2050.96	1
<b>Calculated</b>	ts1	2.34	-1.32	-0.88	0,50	-1.77	1
	ts2	3.32	-3.26	-0.56	0.55	-1.02	1

Table 2: The relative errors of the calculated parameters of the first experiment.

$e_{f1}$	$e_{f2}$	$e_R$	$e_{t1}$	$e_{t2}$
0.25%	1.9%	0.0%	1.4%	1.1%

Table 3: Estimated camera intrinsic parameters for the four sequences

Seq.	Images	$f$	$\epsilon$	$s$	$u_0$	$v_0$
(A)	Image 1	1271.71	0.99	0.03	528.50	334.06
	Image 2	1165.65	1.00	0.07	448.12	291.07
(B)	Image 1	2820.75	0.99	0.01	1542.43	1039.07
	Image 2	2744.83	1.00	0.07	1479.83	990.18
(C)	Image1	2514.79	0.99	0.06	1108.6	1185.65
	Image2	2607.30	1.00	0.08	884.75	1200.05
(D)	Image1	2893.59	1.00	0.16	1140.86	1430.81
	Image2	2967.02	0.99	0.53	1044.57	1416.03

## 6 CONCLUSION

In the present work, we have proposed a new self-calibration method of a CCD camera with variable intrinsic parameters from an unknown scene and based on the use of leak points. We have shown that the determination of intrinsic parameters is possible using only two images. The results are satisfactory in terms of stability, robustness and execution time.

## REFERENCES

Raguram, R., Frahm, J. M., & Pollefeys, M. (2008, October). A comparative analysis of RANSAC techniques leading to adaptive real-time random sample consensus. In *European Conference on Computer Vision* (pp. 500-513). Springer, Berlin, Heidelberg.

Moré, J. J. (1978). The Levenberg-Marquardt algorithm: implementation and theory. In *Numerical analysis* (pp. 105-116). Springer, Berlin, Heidelberg.

Triggs, B. (1998, June). Autocalibration from planar sequences. In *Proceedings of 5th European conference on computer vision*.

Saaidi, A., Halli, A., Tairi, H., & Satori, K. (2008). Self-calibration using a particular motion of camera. *WSEAS Transaction on Computer Research*, 3(5).

Cao, X., Xiao, J., Foroosh, H., & Shah, M. (2006). Self-calibration from turn-table sequences in presence of zoom and focus. *Computer Vision and Image Understanding*, 102(3), 227-237.

Zhao, Y., & Lv, X. D. (2012). An approach for camera self-calibration using vanishing-line. *Information Technology Journal*, 11(2), 276.

Shang, Y., Yue, Z., Chen, M., & Song, Q. (2012). A new method of camera self-calibration based on relative lengths. *Information Technology Journal*, 11(3), 376.

Jiang, Z., & Liu, S. (2012). Self-calibration of varying internal camera parameters algorithm based on quasi-

affine reconstruction. *Journal of Computers*, 7(3), 774-778.

Kluger, F., Ackermann, H., Yang, M. Y., & Rosenhahn, B. (2017, September). Deep learning for vanishing point detection using an inverse gnomonic projection. In *German Conference on Pattern Recognition* (pp. 17-28). Springer, Cham.

Sturm, P. (2002). Critical motion sequences for the self-calibration of cameras and stereo systems with variable focal length. *Image and Vision Computing*, 20(5-6), 415-426.

Gurdjos, P., & Sturm, P. (2003, June). Methods and geometry for plane-based self-calibration. In *2003 IEEE Computer Society Conference on Computer Vision and Pattern Recognition, 2003. Proceedings.* (Vol. 1, pp. I-I). IEEE.

Liu, P., Shi, J., Zhou, J., & Jiang, L. (2003, July). Camera self-calibration using the geometric structure in real scenes. In *Proceedings Computer Graphics International 2003* (pp. 262-265). IEEE.

Zhao, Y., Hu, X., Lv, X., & Wang, H. (2012). Solving the camera intrinsic parameters with the positive tri-prism based on the circular points. *Information Technology Journal*, 11(7), 926.

El Akkad, N., Merras, M., Baataoui, A., Saaidi, A., & Satori, K. (2018). Camera self-calibration having the varying parameters and based on homography of the plane at infinity. *Multimedia Tools and Applications*, 77(11), 14055-14075.

Zhang, W., & Kösecká, J. (2006). Nonparametric estimation of multiple structures with outliers. In *Dynamical Vision* (pp. 60-74). Springer, Berlin, Heidelberg.

Wildenauer, H., & Vincze, M. (2007, September). Vanishing point detection in complex man-made worlds. In *14th International Conference on Image Analysis and Processing (ICIAP 2007)* (pp. 615-622). IEEE.

Toldo, R., & Fusiello, A. (2008, October). Robust multiple structures estimation with j-linkage. In *European conference on computer vision* (pp. 537-547). Springer, Berlin, Heidelberg.